Salt-induced aggregation of stiff polyelectrolytes

2009 J. Phys.: Condens. Matter 21 424111

(http://iopscience.iop.org/0953-8984/21/42/424111)

J. Phys.: Condens. Matter **21** (2009) 424111 (9pp) doi:10.1088/0953-8984/21/42/424111

Salt-induced aggregation of stiff polyelectrolytes

Hossein Fazli[1], **Sarah Mohammadinejad**[1] **and Ramin Golestanian**[2]

[1] Institute for Advanced Studies in Basic Sciences (IASBS), PO Box 45195-1159, Zanjan 45195, Iran
[2] Department of Physics and Astronomy, University of Sheffield, Sheffield S3 7RH, UK

E-mail: fazli@iasbs.ac.ir, sarah@iasbs.ac.ir and r.golestanian@sheffield.ac.uk

Received 2 May 2009
Published 29 September 2009
Online at stacks.iop.org/JPhysCM/21/424111

Abstract
Molecular dynamics simulation techniques are used to study the process of aggregation of highly charged stiff polyelectrolytes due to the presence of multivalent salt. The dominant kinetic mode of aggregation is found to be the case of one end of one polyelectrolyte meeting others at right angles, and the kinetic pathway to bundle formation is found to be similar to that of flocculation dynamics of colloids as described by Smoluchowski. The aggregation process is found to favor the formation of finite bundles of 10–11 filaments at long times. Comparing the distribution of the cluster sizes with the Smoluchowski formula suggests that the energy barrier for the aggregation process is negligible. Also, the formation of long-lived metastable structures with similarities to the raft-like structures of actin filaments is observed within a range of salt concentration.

(Some figures in this article are in colour only in the electronic version)

1. Introduction

It is known that highly charged biological polyelectrolytes (PEs) such as DNA and filamentous actin (F-actin) could attract each other in the presence of multivalent counterions (ions of opposite charge), due to electrostatic correlations [1]. Formation of collapsed bundles of stiff PEs [2, 3], which is believed to play a significant role in biological processes such as cell scaffolding dynamics [4] and motility [5], could arise from these correlations. Experiments always find finite-sized bundles [2, 3] despite the current theoretical understanding of the process of PE bundle formation that predicts a macroscopic phase separation, i.e. an infinitely large bundle [6]. Suggestions like kinetic barriers [7], steric effects [8] and frustration of the local structure with an energy penalty [3, 9] have been presented to explain the difference between the theoretical expectation and the experimental observations. PE bundle formation has also been studied using computer simulation methods [10–13].

The kinetics of bundle formation in multivalent salt solution of actin filaments has been studied experimentally using two different fluorescently labeled filaments and it has been observed that the initial stage of bundle growth tends to saturate when the bundles reach the size of 10–20 filaments and the bundles dynamically exchange filaments with the solution [14]. Also, the dominant kinetic mode of aggregation has been studied using computer simulation methods both in terms of pairs of rods [7, 15, 16] and the bulk solution of stiff PEs [13].

Actin filaments are known that assemble into networks (large crossing angle) or bundles (nearly parallel) depending on their different roles in the cell function, by bundling or cross-linking proteins [17]. Depending on the salt concentration, formation of both networks and dense bundles has also been observed experimentally in multivalent salt solutions of F-actin rods [18]. In a particular range of salt concentrations, a multi-axial liquid crystalline phase of actin rods has been observed in which aggregates such as stacks of raft-like structures form. Formation of novel raft-like aggregates of actin rods in the presence of multivalent salt has been studied recently using a variety of different approaches [19–23]. Considering that aggregates of stiff PEs are dense assemblies of similarly charged rods, such rich complexity is expected due to *frustration* in accommodating strong electrostatic interactions and geometrical constraints simultaneously. Similar effects arising from electrostatic frustration have been studied theoretically in the context of rod-like polyelectrolyte aggregates [24], rod-like polyelectrolyte brushes [25], and star PEs [26].

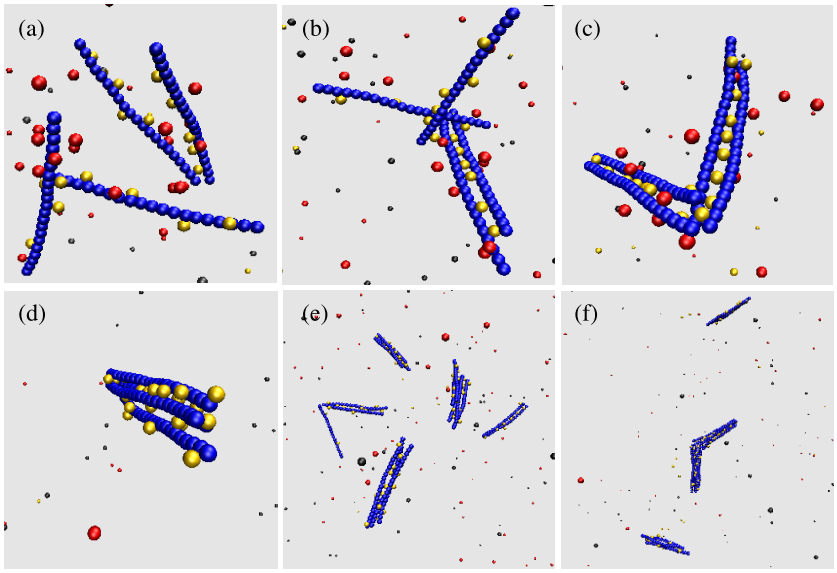

Figure 1. Time lapse snapshots of the system with $N_p = 4$ ((a)–(d)) and $N_p = 16$ ((e), (f)) at $c_{3:1} = 1$. $+3$ salt ions are shown by golden (light) spheres, $+1$ counterions by red (dark), and -1 salt ions by gray spheres. It can be observed that when two filaments or two bundles meet each other the dominant crossing angle is 90°. In the final configuration of the system with $N_p = 4$ all the PEs form a single bundle; however, in the case of $N_p = 16$ two bundles containing 5 and 11 PEs form (the final configuration of $N_p = 16$ rods is not shown here).

We have performed a systematic study of the aggregation process of such PEs, in the form of a combination of bulk solution simulations, calculation of the potential of mean force between a pair of PEs, and studying the evolution of already made structures towards equilibrium in the presence of multivalent salt [13, 23]. Such studies show that PEs in multivalent salt solution undergo an aggregation process with doublets, triplets, etc forming and subsequently feeding into larger clusters. The initial stage of the kinetics leads to the formation of PE bundles that have a clear size selection, up to 10–11 filaments in a range of parameters. These bundles take up all the smaller clusters, and are much more long-lived than the smaller ones, while larger clusters do not seem to appear even when there are a number of these long-lived filament bundles available in the solution for possible aggregation. Time-dependent size distributions of the aggregates follow a Smoluchowski flocculation kinetics with no appreciable energy barrier. The dominant kinetic mode of aggregation is the case of one end of a filament/bundle meeting another filament/bundle either in the middle mostly at right angles (in the form of '⊣') or at one end (in the form of '⟩') before rotating and sliding into a parallel packing (see figure 1). These modes can be understood from energetic considerations by calculating the angle dependence of the potential of mean force between two rods. Simulations of the inverse process of aggregation, i.e. simulation of the evolution of constructed bundles, show that in a range of salt concentrations the kinetics of splitting of large bungles into smaller bundles is similar to the inverse kinetics of aggregation and tendency of the bundles for having finite size is similar to that of the simulations of PE aggregation.

We find that there could be *three* different regimes in the aggregation behavior of stiff PEs in a multivalent salt solution, depending on the salt concentration. When the salt concentration is low, the system does not undergo aggregation because the attraction between PEs is not strong enough to cause it. In an intermediate range of salt concentrations, relatively long-lived structures with special orientational ordering of PEs form. In these scaffold-like structures, PEs are predominantly joined either parallel or perpendicular to each other (see figure 4), which is presumably due to the dominant kinetic mode of aggregation [13]. After sufficiently long time, mutually perpendicular rods in each structure slide against each other and join up in parallel, such that eventually bundles of parallel PEs form. These metastable structures have similarities to the raft-like structures of actin filaments observed experimentally [18]. In the high salt concentration regime, the PEs directly aggregate into bundles of parallel rods and do not exhibit right-angle configurations in their kinetic pathway of aggregation. The angle- and distance-dependent potential of mean force between two similarly charged rigid rods shows that in the low salt concentration regime there is no attraction between rods. In the regime with intermediate values of salt concentration, the interaction between rods is attractive, but in a range of center-to-center separation the preferred angle between the rods is 90°. In this regime, the parallel configuration is preferred only at very close separations. In the high salt concentration regime, the parallel configuration is preferred at all separations and the interaction between parallel rods is attractive.

Constructing raft-like structures and monitoring their subsequent evolution at different salt concentrations (see figure 4) shows that these structures are not stable in the low and high salt concentration regimes: while at low salt concentrations mutual repulsion between rods destroys such structures, at high salt concentrations mutually perpendicular rods slide against each other in a very short time and the raft-like structures change to bundles of parallel rods. In the

intermediate salt concentration regime, raft-like structures are relatively long-lived and their lifetime rapidly increases with the number of rods.

2. The model and the simulation method

2.1. Simulation of the bulk solution of stiff polyelectrolytes

Our simulations are performed with the MD simulation package ESPResSo v.1.8 [27]. In simulations of the bulk solution of stiff PEs, N_p charged stiff chains are considered, each containing $N_m = 21$ spherical monomers of charge $-e$ (electronic charge) and diameter σ. A short-range excluded volume interaction which is described by a shifted Lennard-Jones potential,

$$u_{LJ}(r) = \begin{cases} 4\epsilon\left[\left(\frac{\sigma}{r}\right)^{12} - \left(\frac{\sigma}{r}\right)^{6} + \frac{1}{4}\right] & \text{if } r < r_c \\ 0 & \text{if } r \geqslant r_c, \end{cases} \quad (1)$$

is considered, between monomers, in which ϵ and σ are the usual Lennard-Jones parameters and the cutoff radius is $r_c = 2^{1/6}\sigma$. Neighboring monomers of each chain are bonded to each other via a finite extensible nonlinear elastic (FENE) potential [28],

$$u_{bond}(r) = \begin{cases} -\frac{1}{2}k_{bond}R_0^2 \ln\left[1 - \left(\frac{r}{R_0}\right)^2\right] & \text{if } r < R_0 \\ 0 & \text{if } r \geqslant R_0, \end{cases} \quad (2)$$

with the maximum separation between them being $R_0 = 1.1\sigma$ and $k_{bond} = 50\epsilon/\sigma^2$. The bending rigidity of each PE chain is modeled with a bond angle potential $U_\phi = k_\phi(1 - \cos\phi)$ with $k_\phi = 400\, k_B T$ in which ϕ is the angle between two successive bond vectors along the PE chain. To neutralize the PE charges, $N_c = N_p \times N_m$ monovalent counterions of charge $+e$ are considered. Trivalent salt is also modeled with N_{s+} positive spherical ions with charge $+3e$ and $N_{s-} = 3N_{s+}$ negative ions with charge $-e$. Long-ranged Coulomb interaction is considered between all the charged particles. The MD time step in our simulations is $\tau = 0.01\tau_0$, in which $\tau_0 = \sqrt{m\sigma^2/\epsilon}$ is the MD timescale and m is the mass of the particles.

The temperature is fixed at $k_B T = 1.2\epsilon$ using a Langevin thermostat. To apply periodic boundary conditions, the particle–particle particle-mesh (PPPM) method is used for long-ranged Coulomb interaction in the system. The strength of the electrostatic interaction energy relative to the thermal energy can be quantified using the Bjerrum length $\ell_B = \frac{e^2}{\varepsilon k_B T}$, in which ε is the dielectric constant of the solvent and in our simulations we have used it to fix the value for σ via $\ell_B = 3.2\sigma$. The salt concentration is defined as $c_{3:1} = N_{s-}/N_c$ following [22] (for example $c_{3:1} = 0.5$ means that $N_{s-} = 0.5 \times N_c$) and we use values in the range of $c_{3:1} = 0.5$–1.2. The Debye length $\lambda_D = 6\sigma$ for $c_{3:1} = 1$. Considering that $l_B = 7$ Å in water at room temperature, the value of $l_B = 3.2\sigma$ means that $\sigma = 2.2$ Å and the separation between charged monomers is $a = 2.5$ Å. Using the relation for the effective viscosity of the solvent $\eta \simeq 2.4\sqrt{m\epsilon}/\sigma^2$ (from [29]), an estimate for the microscopic time $\tau_0 \simeq \eta\sigma^3/(2k_B T)$ can be deduced. Using the viscosity of water and room temperature, we obtain $\tau_0 = 1.3$ ps. In the beginning of bulk solution simulations, we fix the PEs in space and leave all the ions to fluctuate around them for 100 000 MD time steps, which is enough to equilibrate the ions for every given configuration of the PEs. After equilibration, we remove the constraint on the PEs and study the aggregation process in the system.

2.2. Calculation of the potential of mean force between two rigid polyelectrolytes

To obtain the dependence of the interaction between two stiff PEs on the angle and the separation between them at different salt concentrations, we do simulations of two rod-like PEs. In these simulations, we consider two rigid PE chains, each composed of $N_m = 21$ similarly charged spherical monomers of diameter σ and charge $-e$, $N_c = 2N_m$ counterions of charge $+e$, and 3-valent salt of concentration $c_{3:1}$. In these simulations, a cubic box of length $L \approx 75\sigma$ is considered that is large enough for avoiding finite size effects. The PEs are fixed on two parallel plates of separation R and the angle between the rods is θ (see the schematic configuration in the inset of figure 5). For each set of values of R, θ, and $c_{3:1}$, the two rods are fixed during the simulation and only the counterions and the salt ions are free to move. After equilibration of the system we calculate the average force on each monomer and obtain the total force and the total torque around the center-to-center line (y-axis) for one of the rods. We integrate the force with respect to the center-to-center distance, R, to obtain the R-dependence of the potential of mean force, and similarly integrate the torque with respect to the angle θ to obtain its θ-dependence (corresponding to rotation around y-axis). We set the zero of the potential of mean force at $R = 7.5\sigma$ for obtaining its R-dependence, and at $\theta = 90°$ in the calculation of its θ-dependence. The other details of the simulation of two rigid PEs are similar to those of bulk solution simulations.

3. Results

3.1. Bundles of parallel polyelectrolytes

3.1.1. Kinetics of aggregation: finite-sized bundles. Simulations of the bulk solution of stiff PEs with different values of N_p ($N_p = 4, 9, 16, 25, 64$) show that in the bulk solutions consisting of four and nine PE rods, in the final equilibrium configuration of the system a single bundle containing all of the PEs forms. However, simulations with larger numbers of PEs, i.e. $N_p = 16, 25$ and 64, show that the growth of the bundles tends to be cut off, or slowed down beyond the time span of the simulation, when there are 10–11 filaments in the bundle, while at the end of the simulation with larger numbers of PEs there are more bundles in the solution, the largest bundle at long times containing at maximum 11 rods. Also it is observed that single PE rods or small bundles of PEs that are going to be added to a bundle of parallel PEs first meet the bundle at right angles and then change their orientation and join it in a parallel configuration. In figure 1

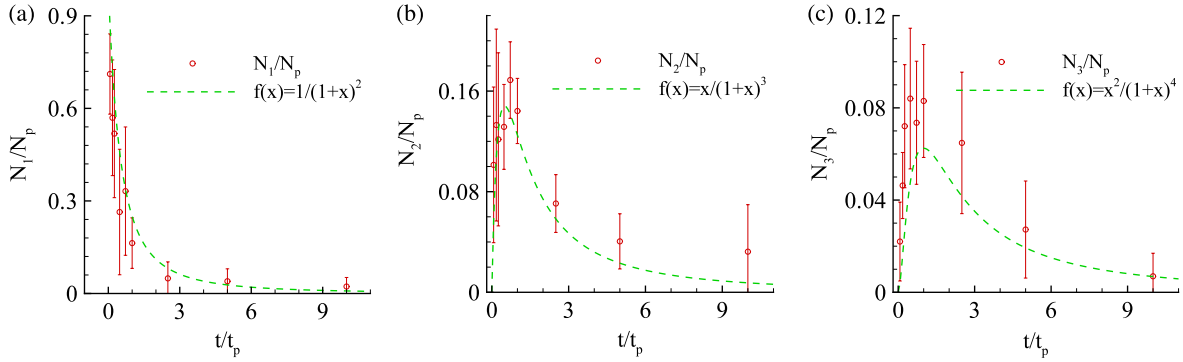

Figure 2. N_k/N_p versus rescaled time t/t_p for (a) $k = 1$, (b) $k = 2$, and (c) $k = 3$, with $W = 1$. Data and error bars are obtained from averaging over sets of data such as those presented in table 1 corresponding to various simulations with identical and differing values of N_p.

snapshots of the system with $N_p = 4$ and 16 PE rods are shown at different simulation times.

Numbers of PE bundles containing different numbers of PE rods can be obtained at different simulation times. For the simulation with $N_p = 25$ PEs, the numbers of PE bundles of different sizes are shown for different times in table 1. In this table, N_k is the number of bundles containing k PEs and for a system with N_p PEs it is subject to the normalization $\sum_k kN_k = N_p$. The largest bundle at long times contains 11 PEs in all the simulations. In the case of $N_p = 16$, two bundles containing 5 and 11 rods remain at long times with no affinity towards each other. The evolution of the clusters and their distribution—as exemplified in table 1 for 25 rods—is found, resembling the aggregation kinetics of colloidal particles [30]. For the case of spherical colloidal particles with short-ranged interactions, Smoluchowski suggested an (approximate) expression for the number of clusters of size k in time t as [30]

$$N_k(t) = \frac{N_p(t/t_p)^{k-1}}{(1+t/t_p)^{k+1}}. \tag{3}$$

Here, the characteristic time is defined as

$$t_p = \frac{\eta W}{n_0 k_B T}, \tag{4}$$

where n_0 is the initial number density of the particles, and $W \simeq e^{E_a/k_B T}$ is an activation factor (up to a numerical coefficient). The values of N_k/N_p for $k = 1, 2$ and 3 obtained from bulk solution simulations as a function of t/t_p are shown in figure 2 with $W = 1$.

Using $\eta \simeq 2.4\sqrt{m\epsilon}/\sigma$, $k_B T = 1.2\epsilon$, $n_0 = 0.001\sigma^{-3}$, and $\tau = 0.01\tau_0 = 0.01\sqrt{m\sigma^2/\epsilon}$ yields $t_p = 2\times10^5\tau W$ in figure 2. In these plots results are compared with the Smoluchowski formula of equation (3) and an agreement can be seen in the range of the error bars. Considering that the clusters do not exceed the maximum size of 10–11 one can conclude that the analogy should be limited to the smaller sizes. Nevertheless, it is remarkable that the same value for t_p gives a good agreement for N_1/N_p, N_2/N_p and N_3/N_p, without even a single fitting parameter being used.

The fact that $W = 1$ seems to provide a reasonable agreement suggests that the PE rods do not experience substantial energy barriers in their 'optimal' kinetic paths in the course of the aggregation. However, one should note that the low optimal energy barrier does not mean that the energetics does not play a role in the kinetics, as the dominant kinetic mode is clearly a result of strong electrostatic interactions.

Table 1. Numbers of PE bundles of different sizes at different MD times for a system with $N_p = 25$ and $c_{3:1} = 1$.

Time ($\times 2000\tau$)	N_1	N_2	N_3	N_4	N_5	N_6	N_{10}
10	18	2	1	0	0	0	0
35	14	4	1	0	0	0	0
42	13	3	2	0	0	0	0
92	10	3	3	0	0	0	0
144	9	3	2	1	0	0	0
158	8	3	1	2	0	0	0
270	7	2	0	2	0	1	0
350	5	3	0	2	0	1	0
400	4	3	0	1	1	1	0
450	4	3	0	0	1	0	1
750	3	2	1	0	1	0	1
1500	2	2	0	1	1	0	1
2000	2	0	0	2	1	0	1
2700	1	0	0	1	0	0	2
2900	0	0	0	0	1	0	2
4000	0	0	0	0	1	0	2

The problem of quantifying the kinetic barrier of the aggregation process is a complicated one, as it is not clear how one can approach it better than just looking at pair potentials. Monitoring the time evolution of the cluster sizes could be a good alternative for capturing the many-body essence of the aggregation process. The typical timescale t_p that is involved in the evolution of the cluster sizes (see equation (4)) has a diffusion-controlled component $\eta/(n_0 k_B T) \sim \ell^3/(LD)$, where $\ell = n_0^{-1/3}$ is the initial average distance between the filaments in the solution, L is the length of the filaments, and D is a filament diffusion coefficient. The second component of t_p comes from the many-body energetics of the system. A comparison of the simulation results for the cluster sizes with the Smoluchowski formulae in figure 2 suggests that the diffusion part is dominant during the early stages of the aggregation until the finite-sized bundles are formed. The fact that the Smoluchowski plots for zero energy barrier are close to the simulation data points shows that the energy barriers

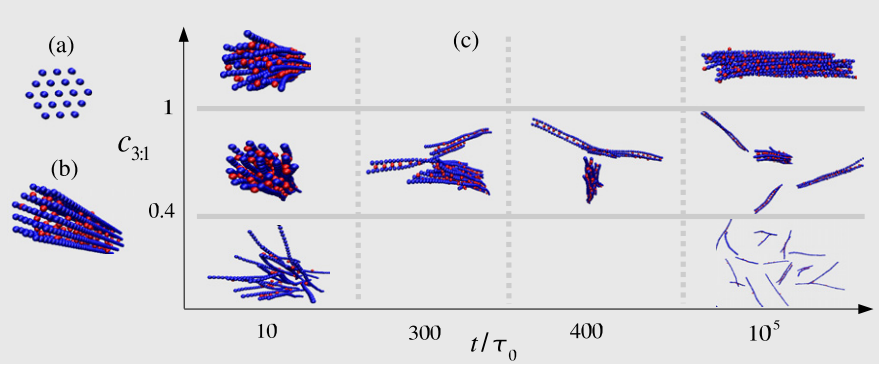

Figure 3. (a) Top view of the initial configuration of $N_p = 19$ parallel PEs arranged on a hexagonal lattice. (b) Side view of the PEs with +3 salt ions after equilibration of the free ions. (c) Sample snapshots from evolution of a constructed bundle containing $N_p = 19$ PEs after equilibration of counterions and the salt ions at different salt concentrations (+3 salt ions are shown by spheres and counterions and −1 salt ions are not shown for clarity).

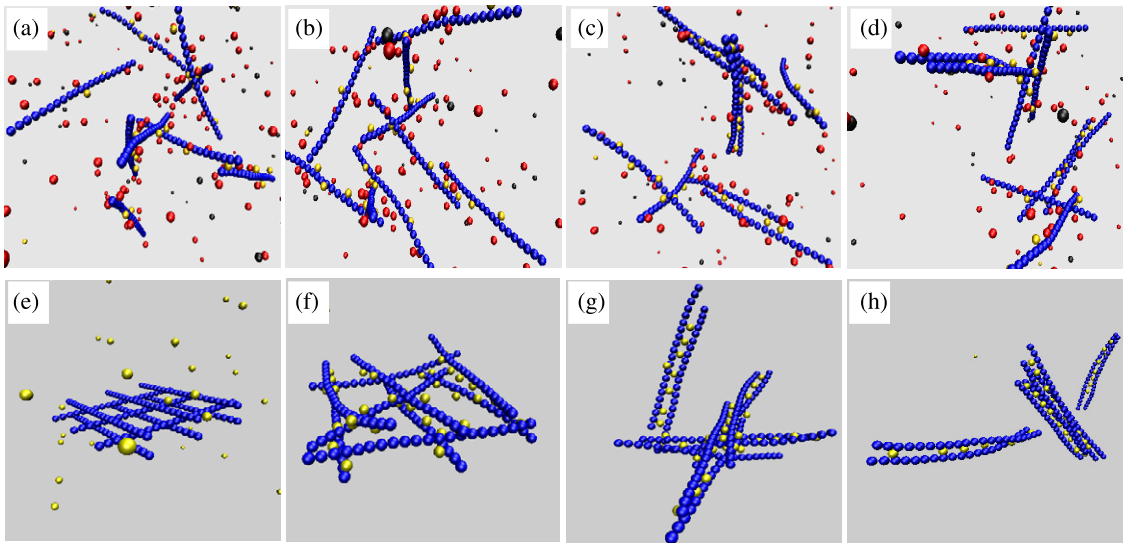

Figure 4. ((a)–(f)) Snapshots of the system containing $N_p = 9$ PEs in solution with 3-valent salt concentration $c_{3:1} = 0.5$ as a function of time. +3 salt ions are shown by golden (light) spheres, +1 counterions by red (dark), and −1 salt ions by gray spheres. Corresponding times of snapshots in units of τ_0: (a) 10, (b) 25, (c) 70, (d) 85. Aggregates of PEs with scaffold-like structures can be seen in the snapshots (c) and (d). Finally, all of the PEs form a single bundle (the last configuration is not shown here). ((e)–(f)) Snapshots from evolution of a raft-like structure formed by $N_p = 9$ PEs in the presence of 3-valent salt of concentration $c_{3:1} = 0.5$. The positive 3-valent salt ions are shown by golden (light) spheres and the negative salt ions and counterions are not shown for clarity. Corresponding times of snapshots in units of τ_0: (e) initial configuration before equilibration of the ions, (f) 250, (g) 550, (h) 700.

have to be small. We chose to plot the zero-energy-barrier form instead of trying to fit the data to the Smoluchowski formula and deduce an energy barrier because we do not know the right prefactors for the different geometry of rods (rather than spheres in the original Smoluchowski solution). However, these prefactors must not differ too much from unity and therefore the argument that the barrier must be small at this stage will be justified from the agreement in figure 2.

3.1.2. Evolution of constructed bundles. For better understanding the process of bundle formation in the solution of stiff PEs, we study the inverse pathway of bundle formation, i.e. evolution of constructed bundles at different concentrations of 3-valent salt. In the beginning of simulation, we arrange the centers of N_p parallel PEs on a hexagonal lattice of spacing $a = 2.2\sigma$ (see figure 3). The PEs are modeled with the same method as was described in section 2.1 and in these simulations each PE consists of $N_m = 36$ charged monomers. Keeping the PEs fixed, we allow the counterions and the salt ions to fluctuate until equilibration is reached. Then we unfix the PEs and study the evolution of the system. From simulations with $N_p = 19$ PEs we find that at low values of salt concentration, $c_{3:1} \leqslant 0.4$, the PEs repel each other and their mutual separations increase rapidly after unfixing. At intermediate salt concentrations, $0.4 < c_{3:1} \leqslant 1$, all of the PEs form a single bundle after removing the constraint, but the bundle is not stable for longer times and its size starts to decrease. The dominant kinetic mode of reduction of the bundle size is similar to the inverse of the dominant mode of aggregation kinetics. The PEs or smaller bundles that are going

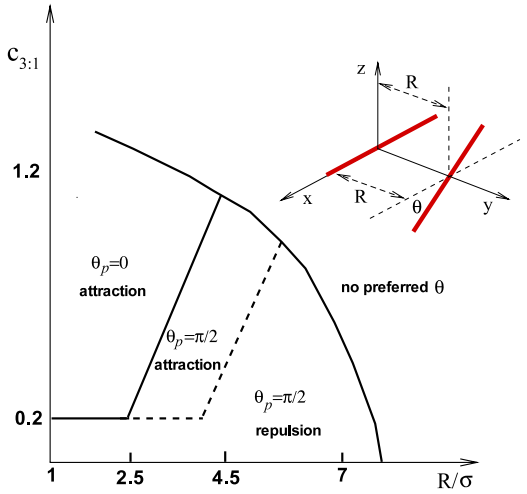

Figure 5. Preferred angle θ_p and type of interaction between two charged rigid rods which are fixed on two parallel plates of separation R, in different regions of $c_{3:1}$–R plane. Inset: schematic configuration of the rods.

to leave the large bundle first slide along it and then leave it at a right angle (see figure 3). With these values of the salt concentration, the largest stable bundles are of equilibrium size 10–12 PEs (for example in figure 3 the initial bundle containing 19 PEs splits into 4 bundles containing 12, 3, 2 and 2 PEs). At high salt concentrations, $c_{3:1} > 1$, the initially formed bundle containing all of the PEs is stable and does not split into smaller bundles at longer times. With such high salt concentrations, simulations with larger numbers of PEs ($N_p = 30$ and 80) also show that the bundle containing all of PEs is stable for very long times ($>10^6\tau_0$).

3.2. Metastable raft-like structures

3.2.1. Scaffold-like aggregates of stiff polyelectrolytes. Bulk solution simulations of stiff PEs in the presence of 3-valent salt show that with changing multivalent salt concentration, three different regimes can exist. At salt concentrations less than a lower value $c_{3:1} \simeq 0.2$ no aggregation is observed in the system. The salt concentration in this regime is lower than its minimum value needed for like-charge attraction between PEs. When a 3-valent salt ion links two monomers from two different PEs to each other, thermal fluctuations separate them again and the system does not undergo an aggregation process. At intermediate salt concentrations $0.2 \leqslant c_{3:1} \leqslant 1.2$, aggregation of PEs happens and the dominant kinetic mode of aggregation is that of one end of one PE meeting others at a right angle. In this regime, long-lived structures of PEs form and in each structure PEs are dominantly joined either parallel or perpendicular to each other (see figure 4(d)). After sufficiently long time, mutually perpendicular PEs in each scaffold-like structure slide against each other and finally form bundles of parallel PEs. The kinetic mode of evolution from scaffold-like structures to bundles is considerably slower than the typical kinetic modes of the system. For example, in a system containing nine PEs, the time that takes for the scaffold-like structure (figure 4(d)) to evolve into the final configuration of a collapsed parallel bundle is greater than the time interval between snapshots (a) and (c) of figure 4, by a factor of at least 6. This suggests that the formation of long-lived scaffold-like structures corresponds to metastable states of the system and the states with bundles of parallel PEs have lower free energies. We have checked that the formation of the metastable structures is independent of the random number sequence used in the simulation, as well as the initial configuration of the PEs. In other words, in the intermediate salt concentration range the relaxation pathway to equilibrium appears to always involve intermediate metastable structures. These structures have similarities to the raft-like structures of actin filaments observed experimentally [18]. In the regime with high values of salt concentration ($c_{3:1} \geqslant 1.2$), we observe a different kinetic mode of aggregation in the system. In this regime, the PEs directly aggregate into bundles of parallel PEs and the salt concentration washes out the right-angle configuration from the kinetic pathway of aggregation. The aggregation process in this regime is considerably faster than that of the regime with intermediate salt concentration.

Calculation of the potential of mean force between two PE rods helps us to better understand the results of the bulk solution results [23]. We calculate the angle-dependent potential of mean force at different values of R. We find that at the lowest value of R in our simulations, $R = 2.5\sigma$, the preferred angle at salt concentrations less than a threshold value $c_{3:1} \simeq 0.2$ is $\theta = 90°$, and at higher salt concentrations, the parallel configuration is preferred. While this is the same result as reported in [22], we find that upon increasing R (from $R = 2.5\sigma$), the threshold value of salt concentration below which $\theta = 90°$ is preferred increases. These results show that in a range of salt concentrations, if we consider two rod-like PEs in the solution at a separation where their effective interaction is appreciable, the interaction potential tends to reorient them to a perpendicular configuration. The preferred orientation is parallel only at very close separations. This could be the origin of the formation of scaffold-like structures in the aggregation of stiff PEs. After the formation of such structures, the PEs are much closer to each other, and will have a chance to discover that the parallel configuration has a lower free energy, and so perpendicular rods eventually reorient themselves and form bundles.

To elaborate further on this issue, we calculate the distance-dependent potential of mean force between two perpendicular rods, which shows that in the presence of 3-valent salt there can be attractive interaction between them at close separations. Moreover, we find that a barrier exists in the potential of mean force, which decreases with increasing salt concentration. This result suggests that within the dominant kinetic mode of aggregation, when two PEs are going to join each other with their ends and at right angles, they experience the lowest possible energy barrier. Using our results on the R- and θ-dependence of the potential of mean force between two rod-like PEs at different salt concentrations, we have shown the preferred crossing angle, θ_p, and the interaction type between two rods at different salt concentrations and center-to-center separations in figure 5. It can be seen in this figure that with increasing salt concentration, the $\theta = \frac{\pi}{2}$ region of the

diagram becomes smaller, until it finally vanishes at $c_{3:1} \simeq 1.0$. Moreover, there is a region in the $c_{3:1}$–R plane for which the preferred angle between the rods is 90° and the interaction is attractive. The existence of such a regime could explain the formation of the scaffold-like structures during the aggregation of PEs. We note that the information extracted from the potential of mean force between a pair of rods on the preferred angle between the rods and whether the interaction is attractive or repulsive does not provide a complete description of the behavior of the system, as the true phase behavior needs to be studied from the global stability (convexity) of the free energy of the system (see e.g. [31] for such a study in the context of columnar DNA aggregates). Such a study, however, will involve making assumptions on the structure of the aggregate, as studying the full infinite dimensional configuration space of a system of N_p rods is not computationally feasible. Instead, we prefer to use the calculation of the potential of the mean force (which is more tractable) to supplement the results obtained from MD simulations that probe the kinetics of the system while relaxing to equilibrium.

3.2.2. Stability of the raft-like structures. The formation of scaffold-like metastable structures during the aggregation of rod-like PEs has similarities to that of the raft-like structures observed experimentally in solutions of F-actin rods with multivalent salt [18]. Since we observe that in an intermediate range of salt concentrations the system is likely to be trapped in metastable states on its way to equilibrium, the question naturally arises of how this finding might have relevance to experiments on highly charged rod-like PEs such as F-actin in the presence of multivalent salt. The formation of aggregates from single filaments distributed randomly in the solution as the initial configuration is controlled by a timescale that has two components, namely the time that it takes the filaments to find each other through diffusion and the time that it takes to overcome energetic barriers. Since the diffusion component of the characteristic relaxation time could be substantial for dilute solutions, having long relaxation times does not necessarily mean that large energetic barriers impede the formation of equilibrium structures [13, 14]. To eliminate the diffusion component of the aggregation time and focus specifically on the energetic barriers in the dynamics of the system, we can study the evolution of already made complexes towards equilibrium. While strictly speaking this corresponds to a different kinetic pathway, one can imagine that a similar process of disentanglement of the interacting filaments will be followed in the aggregation kinetics, on the way to equilibrium. Therefore, measuring the relaxation times of already formed structures could provide a direct quantitative measure of the kinetics of the metastable state of the system. To this end, we study systematically the stability and time evolution of raft-like aggregates under various conditions.

We construct raft-like structures of stiff PEs at different salt concentrations, and fix them at the beginning of the simulation (see figures 4(e)–(h)) while the counterions and the salt ions are allowed to fluctuate. After the equilibration of the free ions, we release the constraints on the polyelectrolyte rods and follow the evolution of the system. We find that in the low salt concentration regime thermal fluctuations destroy these structures in a short time. In fact, in this regime, there is not enough salt in the system for like-charge attraction between PEs to appear and the electrostatic repulsion between the rods make such structures unstable. In the high salt concentration regime also the raft-like structures have a fast evolution and considerably short lifetime. In this regime mutually perpendicular rods slide against each other in a short time and the structure changes to bundles of parallel rods.

In the regime with intermediate salt concentration, however, the system has a different evolution. In this regime we find that the raft-like structures are considerably long-lived and it takes a long time for the fluctuations to destroy them. The system finally finds the lower free energy state in which bundles of parallel PEs are formed. In this regime, the stability of raft-like structures increases with increasing salt concentration. A time lapse view of the system with $N_p = 9$ rods is shown in figure 4.

To help quantify the stability of the raft-like structures, we study the dependence of the time of evolution of the structures towards bundles of parallel PEs as a function of the size of these structures while keeping the volume density of the filaments constant (by increasing the size of the simulation box with increasing number of filaments). The evolution time t_e is defined as the time it takes for a raft-like structure containing N_p PEs to change to bundles of PEs; for example the time interval between snapshots (e) and (h) of figure 4. The evolution time t_e as a function of the number of PEs in the raft-like structure N_p is shown in figure 6(a). The data points in this figure are obtained by averaging over five different runs of the system. In this figure, $N_p = 9$ corresponds to three mutually perpendicular layers and each layer contains three parallel rods (see figure 4). Similarly, $N_p = 15, 20, 25, 30, 40$ respectively correspond to 3, 4, 5, 6 and 8 layers and each layer contains five parallel rods. The characteristic evolution time t_e can be thought of as the time that it takes for the raft-like structure to disentangle the filaments that strongly interact with each other via frustrated electrostatic interactions, and as can be seen in figure 6(a) it increases with increasing size of the raft-like structure N_p. The increase is faster than linear, and can be approximated as a power law with an exponent of about 2.7 (see the inset of figure 6(a) for a log–log plot of t_e versus N_p), although the numerical data are not over a sufficiently large domain, so the power law nature can be verified. The characteristic relaxation time of the system as a function of the number of filaments (for a fixed volume density of single filaments) can be used to estimate the N_p-dependence of the energy barrier (or activation energy) E_a for the transition between the raft-like structure and the equilibrium structure. Assuming a form of $t_e(N_p) = t_0 e^{E_a(N_p)/k_B T}$, where t_0 is a microscopic timescale that does not depend on the number of filaments, we can calculate relative changes in the activation energy as shown in figure 6(b). While the plot in figure 6(b) clearly shows that the energy barrier increases with the number of filaments, more studies are necessary to determine whether this trend will continue or ultimately level off for systems with a considerably larger number of filaments.

Using the estimate for the microscopic timescale $\tau_0 = 1.3$ ps, we find that for 9 rods the relaxation time is $\sim$1 ns

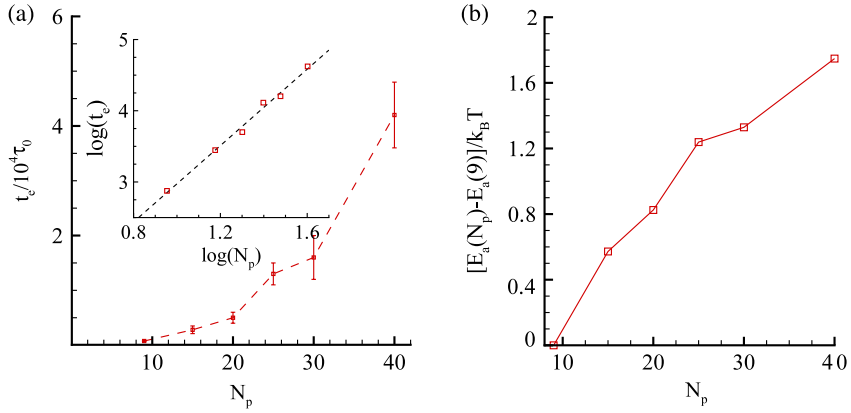

Figure 6. (a) Time of evolution of raft-like structures to bundles of parallel PEs as a function of N_p, the number of PEs forming these structures. Error bars are obtained from averaging over five runs of the simulation with different random number sequences. Inset: log–log plot of t_e versus N_p and a line with the slope of 2.7 (dashed line). (b) Activation energy extracted from (a) as a function of N_p.

and for 40 rods it is ∼0.1 μs. To obtain a crude estimate for the typical relaxation times corresponding to realistic experimental cases [18], we can extrapolate the empirical scaling law to $N_p \sim 10^7$, which yields $t_e \sim 10^7$ s. This estimate suggests that the time for which the system could be trapped in a metastable state could be considerably long compared to typical observation times, for a system like F-actin. Further studies are necessary to determine whether the super-linear increase of the relaxation time as a function of the number of filaments persists for such large numbers present in the experiments on F-actin.

4. Discussion

Experiments seem to tell us consistently that independently of the structure, aggregation of highly charged rod-like polyelectrolytes always leads to the formation of finite bundles. The results presented here, which we hope will shed some light on this puzzling behavior, can be summarized as follows. (1) Our simulations seem to indicate that electrostatic correlations alone are enough to lead to the formation of finite bundles within our finite observation time, and there is no need, for example, for additional structural features such as chirality and structural/geometrical/elastic frustration, or hindrance of counterions due to their finite size. (2) The time it takes for these aggregates to form is long, but it is mostly controlled by the diffusion-limited component of the aggregation kinetics and not by large kinetic energetic barriers. Both our simulation results and an analysis of the experimental data available on actin [14] show that long relaxation times (even of the order of hours for actin) would still imply energetic barriers of order $\sim k_B T$ which are negligible for this system. Therefore, we find that large energetic kinetic barriers cannot be the cause of the formation of finite bundles. (3) We cannot yet make a statement about the true nature of the finite bundles and whether they are in thermodynamic equilibrium or in a kinetically trapped state, from computer simulations of finite observation time. We have followed two alternative routes and monitored the kinetics of aggregation of freely dispersed filaments and segregation of already formed structures such as bundles and rafts. With the already formed large bundles, we find that within our finite observation time the bundles split into smaller 'more stable' ones in an intermediate salt concentration while they seem to stay stable at higher concentrations. This is generally in line with the observation of [12] where also both possibilities are observed. While the alternative kinetic pathway of starting with an already formed bundle is a very good added piece for this puzzle, we should note that an already formed bundle is actually deeper in a potential well and the kinetic barrier to be dissolved—if indeed the equilibrium state is finite bundles—will be considerably higher. In other words, aggregating rods from a disperse solution should feel a much weaker kinetic barrier, and therefore have a better chance of finding the equilibrium state during our finite simulation time. Needless to say, much more needs to be done to understand this complex aggregation more thoroughly and determine the true nature of the finite-sized bundles.

Acknowledgments

We are grateful to C Holm and Y Levin for helpful discussions and for suggestions regarding parts of this work.

References

[1] Holm C, Kekicheff P and Podgornik R 2001 *Electrostatic Effects in Soft Matter and Biophysics* (Dordrecht: Kluwer)
Levin Y 2002 *Rep. Prog. Phys.* **65** 1577
Boroudjerdi H, Kim Y-W, Naji A, Netz R R, Schlagberger X and Serr A 2005 *Phys. Rep.* **416** 129
[2] Bloomfield V A 1991 *Biopolymers* **31** 1471
Podgornik R, Rau D and Parsegian V A 1994 *Biophys. J.* **66** 962
Bloomfield V A 1996 *Curr. Opin. Struct. Biol.* **6** 334
Tang J X and Janmey P A 1996 *J. Biol. Chem.* **271** 8556
Tang J X *et al* 1997 *Biochemistry* **36** 12600
Lyubartsev A P *et al* 1998 *Phys. Rev. Lett.* **81** 5465
Butler J C *et al* 2003 *Phys. Rev. Lett.* **91** 028301
Needleman D J *et al* 2004 *Proc. Natl Acad. Sci. USA* **101** 16099
[3] Angelini T E *et al* 2003 *Proc. Natl Acad. Sci. USA* **100** 8634
[4] Pollard T D and Cooper J A 1986 *Annu. Rev. Biochem.* **55** 987

Jamney P A *et al* 1990 *Nature* **345** 89
Isenberg G 1996 *Semin. Cell Div. Biol.* **7** 707
Borukhov I *et al* 2005 *Proc. Natl Acad. Sci. USA* **102** 3673
[5] Karakozova M *et al* 2006 *Science* **313** 192
[6] Ha B-Y and Liu A J 1998 *Phys. Rev. Lett.* **81** 1011
Shklovskii B I 1999 *Phys. Rev. Lett.* **82** 3268
Huang C-I and Olvera de la Cruz M 2002 *Macromolecules* **35** 976
[7] Ha B-Y and Liu A J 1999 *Europhys. Lett.* **46** 624
[8] Henle M L and Pincus P A 2005 *Phys. Rev.* E **71** 060801(R)
[9] Grason G M and Bruinsma R F 2007 *Phys. Rev. Lett.* **99** 098101
[10] Stevens M 1999 *Phys. Rev. Lett.* **82** 101
[11] Limbach H J, Sayar M and Holm C 2004 *J. Phys.: Condens. Matter* **16** S2135
[12] Sayar M and Holm C 2007 *Europhys. Lett.* **77** 16001
[13] Fazli H and Golestanian R 2007 *Phys. Rev.* E **76** 041801
[14] Lai G H, Zribi O V, Coridan R, Golestanian R and Wong G C L 2007 *Phys. Rev. Lett.* **98** 187802
[15] Yu X and Carlsson A E 2004 *Biophys. J.* **87** 3679
[16] Nguyen T T and Shklovskii B I 2002 *Phys. Rev.* E **65** 031409
[17] Lodish H, Berk A, Zipursky S L, Matsudaria P, Baltimore D and Darnell J 2007 *Molecular Cell Biology* 6th edn (New York: Freeman)
[18] Wong G C L, Lin A, Tang J X, Li Y, Janmey P A and Safinya C R 2003 *Phys. Rev. Lett.* **91** 018103
[19] Borukhov I and Bruinsma R F 2001 *Phys. Rev. Lett.* **87** 158701
[20] Stilck J, Levin Y and Arenzon J J 2002 *J. Stat. Phys.* **106** 287–99
[21] Borukhov I, Bruinsma R F, Gelbart W M and Liu A J 2005 *Proc. Natl Acad. Sci. USA* **102** 3673
[22] Lee K C, Borukhov I, Gelbert W M, Liu A J and Stevens M J 2004 *Phys. Rev. Lett.* **93** 128101
[23] Mohammadinejad S, Fazli H and Golestanian R 2009 *Soft Matter* **5** 1522
[24] Fazli H, Golestanian R and Kolahchi M R 2005 *Phys. Rev.* E **72** 011805
[25] Fazli H, Golestanian R, Hansen P L and Kolahchi M R 2006 *Europhys. Lett.* **73** 429
[26] Konieczny M and Likos C N 2007 *Soft Matter* **3** 1130
[27] Limbach H J, Arnold A, Mann B A and Holm C 2006 *Comput. Phys. Commun.* **174** 704
[28] Grest G S and Kremer K 1986 *Phys. Rev.* A **33** 3628
[29] Dünweg B and Kremer K 1991 *Phys. Rev. Lett.* **66** 2996
[30] Russel W B, Saville D A and Schowalter W R 1988 *Colloidal Dispersions* (Cambridge: Cambridge University Press)
[31] Harreis H M, Kornyshev A A, Likos C N, Löwen H and Sutmann G 2002 *Phys. Rev. Lett.* **89** 018303
Harreis H M, Likos C N and Löwen H 2003 *Biophys. J.* **84** 3607